

Instability of Fulde-Ferrell-Larkin-Ovchinnikov states in three and two dimensions

Jibiao Wang, Yanming Che, Leifeng Zhang and Qijin Chen*

*Department of Physics and Zhejiang Institute of Modern Physics,
Zhejiang University, Hangzhou, Zhejiang 310027, China and*

Synergetic Innovation Center of Quantum Information and Quantum Physics, Hefei, Anhui 230026, China

(Dated: October 4, 2018)

The exotic Fulde-Ferrell-Larkin-Ovchinnikov (FFLO) states have been actively searched for experimentally since the mean-field based FFLO theories were put forward half a century ago. Here we investigate the stability of FFLO states against unavoidable pairing fluctuations, and conclude that FFLO superfluids cannot exist due to their intrinsic instability in three and two dimensions. This explains their absence in experimental observations in both condensed matter systems and the most recent, more promising ultracold atomic Fermi gases with a population imbalance.

The exotic Fulde-Ferrell-Larkin-Ovchinnikov (FFLO) states, which were first predicted by Fulde and Ferrell [1] (FF) and Larkin and Ovchinnikov [2] (LO) in an s -wave superconductor in the presence of a Zeeman field over fifty years ago, have attracted enormous attention in condensed matter physics [3], including heavy-fermion [4, 5], organic [6] and high T_c superconductors [7], nuclear matter [8] and color superconductivity [9], and, more recently, in ultracold Fermi gases [10]. Conventional BCS superfluidity originates from Bose-Einstein condensation (BEC) of Cooper pairs at zero momentum. In contrast, in these exotic states, Cooper pairs condense either at a finite momentum \mathbf{q} , with an order parameter of the form of a plane-wave $\Delta(\mathbf{r}) = \Delta_0 e^{i\mathbf{q}\cdot\mathbf{r}}$ or at momenta $\pm\mathbf{q}$, with an order parameter of the form of a standing wave $\Delta(\mathbf{r}) = \Delta_0 \cos(\mathbf{q}\cdot\mathbf{r})$ for the FF and LO states, respectively.

These exotic superfluids have been actively searched for over the past half century. In condensed matter systems, the strongest signatures of FFLO states come from heavy fermion UPd₂Al₃ [11], CeRu₂ [12] and CeCoIn₅ [4, 5]. However, Refs. [11] and [12] were shown to be inconsistent with theory [13, 14]. Radovan *et al.* [4] assumed an incorrect FFLO wavevector direction perpendicular to the highly two-dimensional Fermi surface, and their claim seemed also to have been dismissed recently by Kenzelmann *et al.* [5], who also noticed discrepancies between theory and their own experimental observations. Thus far, *there has been no solid experimental evidence for the FFLO states from condensed matter systems.*

With the easy tunability of various control parameters, including interaction, dimensionality, population imbalance as well as mass imbalance [15, 16], ultracold Fermi gases have provided a much greater opportunity and given rise to a high expectation for finding the FFLO states. Despite many theoretical studies in this regard, both in a 3D homogeneous case [17–22] and in a trap [23–25], the experimental search for these exotic states in atomic Fermi gases has not been successful [26, 27]. There have also been theoretical studies of FFLO states in more complex systems, such as Fermi-Fermi mixtures [22, 28, 29] or optical lattices [30]. However, exper-

imentally, the superfluid regime in these complex systems has yet to be accessed.

In this paper, we will reveal the deep reason why the FFLO states have not been observed experimentally. Here we investigate the stability of FFLO states against ubiquitous pairing fluctuations, first with simple arguments based on general physical grounds, and then using a concrete pairing fluctuation theory [15, 31], which has been applied successfully to the BCS-BEC crossover physics. We find that FFLO states are indeed intrinsically unstable at any finite temperature T due to pairing fluctuations. This conclusion can be drawn using rival approaches of pairing fluctuation theories as well. We shall mainly work with the 3D case and readily generalize to 2D. We note that both the FF and LO states as well as higher order crystalline states in the literature are essentially constructed at the mean field level, and their stability has never been *properly* tested against pairing fluctuations.

Now consider a single minority fermion in the presence of a majority Fermi sphere in homogeneous 3D continuum, assuming an equal mass for both majority and minority fermions. When the pairing strength is weak, the ground state is a polaron in the Fermi sea. When the interaction becomes just strong enough, the minority atom will pair with a majority atom near the Fermi surface to form a (meta-)stable pair. To minimize the system energy, the pair dispersion will reach a minimum at a finite momentum of $q \approx k_F$, where k_F is the majority Fermi wave vector [32]. Similar things will happen for a two component gas with a high population imbalance. For weak interactions, the ground state will be minority polarons moving in the majority Fermi sea. For very strong interactions in the BEC regime, a polarized Sarma superfluid will emerge at low T . For intermediate pairing strengths, where the majority Fermi surface still exists, (meta-)stable Cooper pairs will form at finite T , with a dispersion minimizing at a finite momentum q . These pairs will first form in the normal state without phase coherence, moving in all possible directions. As T decreases, the system will either phase separate into a 50-50 mixture forming a BCS superfluid plus a majority normal Fermi gas, or try to enter an FF or LO state. Now that the pair dispersion minimizes at a finite momentum, i.e., on

a 2D spherical surface \mathbb{S}^2 in the momentum space, one finds immediately that no condensation is needed at any finite T , in order to satisfy the pair density constraint. Alternatively, the pairing fluctuations will destroy any tendency of Bose condensation of the pairs.

The key here is that in the momentum space, FFLO states can be regarded as condensation of pairs (at finite momenta) whose energy minimizes on a 2D sphere \mathbb{S}^2 . Such a 2D Bose surface for the pair dispersion has a finite density of states (DOS), leading to an effective reduction of the dimensionality for the pairs from 3D to 2D, so that these fluctuations will destroy any attempt for condensation, in accord with the Mermin-Wagner theorem. This argument can be readily extended to the case of an optical lattice, where the 2D sphere is to be replaced by a 2D constant-energy surface.

Next we examine what would happen if one forces a symmetry breaking into an FFLO state at low T with a wavevector \mathbf{q} pointing in the symmetry breaking direction, as in a mean-field treatment. To this end, we proceed with a concrete theoretical formalism of pairing fluctuations in two-component homogeneous Fermi gases with a population imbalance in 3D continuum. We begin by presenting the mean-field solutions, and then show that the mean-field FFLO phase will eventually be destroyed by pairing fluctuations. We shall first restrict ourselves to regular symmetry breaking, i.e., with only one wavevector \mathbf{q} , which corresponds to the FF states. As usual, we work a short-range contact potential of strength $U < 0$. In this assumed FF phase, momentum \mathbf{k} pairs with $\mathbf{q} - \mathbf{k}$ and thus the condensed Cooper pairs have a nonzero center-of-mass momentum \mathbf{q} . Note that setting $\mathbf{q} = 0$ would give us the formalism for the Sarma superfluid state. The dispersion of free atoms is given by $\xi_{\mathbf{k},\sigma} = \mathbf{k}^2/2m_\sigma - \mu_\sigma$, where m_σ and μ_σ are the mass and chemical potential for (pseudo)spin $\sigma = \uparrow, \downarrow$, respectively. We set the volume $V = 1$, $\hbar = k_B = 1$.

In order to self-consistently treat the pairing fluctuation effects, we use a pairing fluctuation theory previously developed [31] for treating the pseudogap phenomena in high T_c superconductors, which has later been extended successfully to address a variety of ultracold Fermi gas experiments without [15, 33, 34] and with population [35, 36] and/or mass imbalances [37, 38]. Within this theory, the BCS mean-field solution of the FF states can be obtained from the combined gap equation and number equations by neglecting the pseudogap equation. In addition, in the superfluid phase, the effective chemical potential of the pairs μ_{pair} vanishes, which guarantees that the pair excitation energy is *not* gapped in the superfluid phase.

Now we shall present our self-consistent equations for the mean-field solution from this theory. Since the pair dispersion minimizes at $\mathbf{q} \neq 0$ for the FF states, the Thouless criterion for pairing instability now reads $t_{pg}^{-1}(0, \mathbf{q}) = U^{-1} + \chi(0, \mathbf{q}) = 0$, with $t_{pg}(P)$ being the T -matrix, $\chi(P) = \sum_{K,\sigma} G_{0\sigma}(P - K)G_{\bar{\sigma}}(K)/2$ the pair susceptibility, $G_0(K)$ and $G(K)$ the bare and full Green's functions, respectively, and $G_{0\sigma}^{-1}(K) = i\omega_n - \xi_{\mathbf{k},\sigma}$. (Here spin $\bar{\sigma}$ is the opposite of spin σ). We refer the readers to Ref. [38] for the convention

on notations. The self-energy [15] takes approximately the simple BCS-like form, $\Sigma_\sigma(K) = -\Delta^2 G_{0\bar{\sigma}}(Q - K)$, with $Q \equiv (0, \mathbf{q})$. Therefore, we have

$$G_\uparrow(K) = \frac{u_{\mathbf{k}}^2}{i\omega_n - E_{\mathbf{k},\uparrow}} + \frac{v_{\mathbf{k}}^2}{i\omega_n + E_{\mathbf{k},\downarrow}}, \quad (1a)$$

$$G_\downarrow(K) = \frac{u_{\mathbf{q}-\mathbf{k}}^2}{i\omega_n - E_{\mathbf{q}-\mathbf{k},\downarrow}} + \frac{v_{\mathbf{q}-\mathbf{k}}^2}{i\omega_n + E_{\mathbf{q}-\mathbf{k},\uparrow}}, \quad (1b)$$

where $u_{\mathbf{k}}^2 = (1 + \xi_{\mathbf{k}\mathbf{q}}/E_{\mathbf{k}\mathbf{q}})/2$, $v_{\mathbf{k}}^2 = (1 - \xi_{\mathbf{k}\mathbf{q}}/E_{\mathbf{k}\mathbf{q}})/2$, $E_{\mathbf{k}\mathbf{q}} = \sqrt{\xi_{\mathbf{k}\mathbf{q}}^2 + \Delta^2}$, and $E_{\mathbf{k},\uparrow} = E_{\mathbf{k}\mathbf{q}} + \zeta_{\mathbf{k}\mathbf{q}}$, $E_{\mathbf{k},\downarrow} = E_{\mathbf{k}\mathbf{q}} - \zeta_{\mathbf{k}\mathbf{q}}$, $\xi_{\mathbf{k}\mathbf{q}} = (\xi_{\mathbf{k},\uparrow} + \xi_{\mathbf{q}-\mathbf{k},\downarrow})/2$, $\zeta_{\mathbf{k}\mathbf{q}} = (\xi_{\mathbf{k},\uparrow} - \xi_{\mathbf{q}-\mathbf{k},\downarrow})/2$. Here the quasiparticle dispersion $E_{\mathbf{k},\sigma}$ may not be gapped. In the presence of mass imbalance, $u_{\mathbf{k}}^2 \neq u_{\mathbf{q}-\mathbf{k}}^2$, unlike the equal-mass case. With the BCS form for the Green's functions Eq. (1), the Thouless criterion becomes

$$\frac{m_r}{2\pi a} = \sum_{\mathbf{k}} \left[\frac{1}{2\epsilon_{\mathbf{k}}} - \frac{1 - 2\bar{f}(E_{\mathbf{k}\mathbf{q}})}{2E_{\mathbf{k}\mathbf{q}}} \right], \quad (2)$$

where $\epsilon_{\mathbf{k}} = k^2/4m_r$ with reduced mass m_r . Here $\bar{f}(x) = [f(x + \zeta_{\mathbf{k}\mathbf{q}}) + f(x - \zeta_{\mathbf{k}\mathbf{q}})]/2$, and $f(x)$ is the Fermi distribution function. Note that U has been replaced by the s -wave scattering length a via $U^{-1} = m_r/2\pi a - \sum_{\mathbf{k}} 1/2\epsilon_{\mathbf{k}}$.

From the number constraint $n_\sigma = \sum_K G_\sigma(K)$, we can get the number density $n = n_\uparrow + n_\downarrow$ and density difference $\delta n \equiv n_\uparrow - n_\downarrow$,

$$n = \sum_{\mathbf{k}} \left[\left(1 - \frac{\xi_{\mathbf{k}\mathbf{q}}}{E_{\mathbf{k}\mathbf{q}}}\right) + 2\bar{f}(E_{\mathbf{k}\mathbf{q}}) \frac{\xi_{\mathbf{k}\mathbf{q}}}{E_{\mathbf{k}\mathbf{q}}} \right], \quad (3)$$

$$\delta n = \sum_{\mathbf{k}} \left[f(E_{\mathbf{k},\uparrow}) - f(E_{\mathbf{k},\downarrow}) \right]. \quad (4)$$

The population imbalance is defined as $\eta = \delta n/n$.

The FFLO wavevector \mathbf{q} can be determined via $\frac{\partial \chi(0, \mathbf{p})}{\partial \mathbf{p}} \Big|_{\mathbf{p}=\mathbf{q}} = 0$, which is equivalent to minimizing the thermodynamic potential Ω_S with respect to \mathbf{q} [22]. Then we have

$$\sum_{\mathbf{k}} \left[\frac{\mathbf{k}}{m_\uparrow} (n_{\mathbf{k}\mathbf{q}} + \delta n_{\mathbf{k}\mathbf{q}}) + \frac{\mathbf{q} - \mathbf{k}}{m_\downarrow} (n_{\mathbf{k}\mathbf{q}} - \delta n_{\mathbf{k}\mathbf{q}}) \right] = 0, \quad (5)$$

where $n_{\mathbf{k}\mathbf{q}}$ and $\delta n_{\mathbf{k}\mathbf{q}}$ are given by the summands of Eqs. (3) and (4), respectively.

Equations (2)-(5) form a closed set, and can be used to solve for the mean-field solution of the one-plane-wave FFLO state, e.g., for $(\mu_\uparrow, \mu_\downarrow, T_c, \mathbf{q})$ with $\Delta = 0$, and for $(\mu_\uparrow, \mu_\downarrow, \Delta, \mathbf{q})$ at $T < T_c$. Dropping Eq. (5) and setting $\mathbf{q} = 0$ would lead to mean-field equations for homogeneous Sarma phases.

At the mean-field level, the FFLO solutions may be further restricted by the stability condition against phase separation (PS) [17, 39, 40],

$$\frac{\partial^2 \Omega_S}{\partial \Delta^2} \frac{\partial^2 \Omega_S}{\partial \mathbf{q}^2} - \left(\frac{\partial^2 \Omega_S}{\partial \Delta \partial \mathbf{q}} \right)^2 > 0. \quad (6)$$

With the mean-field solutions, one can extract the pair dispersion $\Omega_{\mathbf{p}}$ via a Taylor expansion of the inverse T -matrix

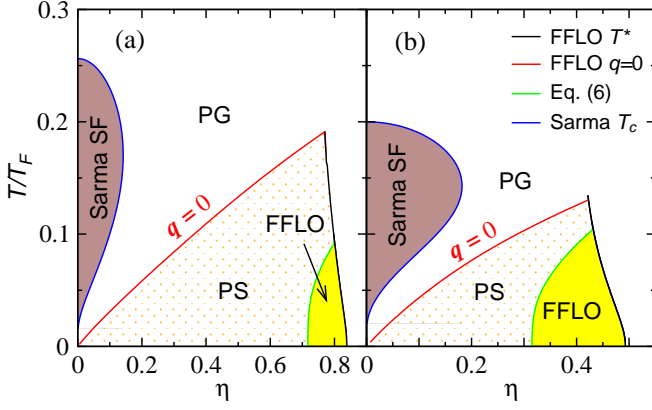


Figure 1. T - η phase diagram of a homogeneous Fermi gas with equal mass at (a) $1/k_F a = 0$ and (b) -0.5 , corresponding to unitary and near-BCS cases, respectively. Here “PG” and “PS” indicate pseudogapped normal state and phase separation, respectively. An FFLO phase (yellow shaded) exists in the low T and relatively high η regime, while they become unstable against phase separation in the dotted region. A beyond-mean-field Sarma superfluid lives in the intermediate T and low η regime (brown shaded region).

[15], i.e., $t_{pg}^{-1}(\Omega, \mathbf{p}) \approx a_0(\Omega - \Omega_{\mathbf{p}} + \mu_{pair}) = 0$, after analytic continuation, where $\Omega_{\mathbf{p}} = -[\chi(0, \mathbf{p}) - \chi(0, \mathbf{q})]/a_0 \approx B_{\parallel}(p_{\parallel} - q)^2 + B_{\perp}p_{\perp}^2$ near $\mathbf{p} = \mathbf{q}$. The coefficients a_0 , B_{\parallel} , B_{\perp} , and μ_{pair} can be readily derived during the expansion, with $\mu_{pair} = 0$ at $T \leq T_c$, and $\mu_{pair} < 0$ above T_c . Here the subscripts “ \parallel ” and “ \perp ” denote parallel with and perpendicular to the \mathbf{q} direction, respectively.

One may also compute the pseudogap, if well defined (as in a Sarma phase), via

$$\Delta_{pg}^2 \equiv - \sum_P t(P) = a_0^{-1} \sum_{\mathbf{p}} b(\Omega_{\mathbf{p}}), \quad (7)$$

where $b(x)$ is the Bose distribution function. Just as the pairing fluctuations tend to destroy the condensate, the presence of Δ_{pg} serves to deplete the order parameter Δ_{sc} from the total excitation gap via $\Delta_{sc}^2 = \Delta^2 - \Delta_{pg}^2$. In this case, pairing fluctuations will reduce T_c from its mean-field value to a lower temperature as determined by $\Delta_{pg} = \Delta$.

For an equal-mass case, we take the majority (minority) species as spin up (down) in our numerics. For Fermi-Fermi mixtures, we take the heavy (light) species to be spin up (down). In both cases, we take Fermi momentum $k_F = (3\pi^2 n)^{1/3}$, and define Fermi temperature as $T_F = k_F^2/2m$, with $m = (m_{\uparrow} + m_{\downarrow})/2$.

We first present in Fig. 1 the calculated mean-field T - η phase diagram for a homogeneous Fermi gas with equal mass for the (a) unitary and (b) near-BCS cases, respectively. Pairing takes place below the pairing temperature T^* (black solid curve), where a pseudogap (PG) starts to emerge. Here we focus on the FFLO phase, not showing the boundary separating the pseudogap state and the high T normal phase, which is a crossover rather than a true phase transition. A mean-field FFLO state in the low T and relatively high η regime for both

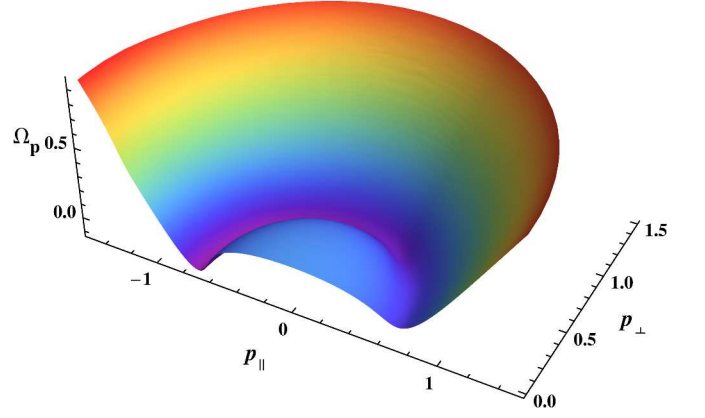


Figure 2. Typical pair dispersion $\Omega_{\mathbf{p}}$ in the FFLO phases in Fig. 1. Shown here is the unitary case with $\eta = 0.75$ and $T/T_F = 0.01$. The color coding is such that $\Omega_{\mathbf{p}}$ increases with the wavelength of the light. The units for energy and momentum are E_F and k_F , respectively.

cases. For lower η , the FFLO states become unstable against phase separation (PS) at low T (dotted region), and these two phases are divided by the green line, as determined by the stability condition Eq. (6). The red line denotes where \mathbf{q} drops to zero. We also show the stable beyond-mean-field Sarma superfluid (SF) phase (brown area) at intermediate T , as found previously [17, 35]. At the mean-field level, the PG phase would be called the Sarma superfluid as well.

The phase diagram of the near-BEC case (say, $1/k_F a = 0.1$) is similar but with a smaller phase space area for the FFLO states, which eventually shrinks to zero towards the BEC regime. The counterpart phase diagrams for Fermi-Fermi mixtures such as ${}^6\text{Li}$ - ${}^{40}\text{K}$ can be found in Ref. [22].

As a representative example, we next show in Fig. 2 a 3D plot of the pair dispersion $\Omega_{\mathbf{p}}$ in the FFLO phases. We pick the unitary case in Fig. 1, with $\eta = 0.75$ and $T/T_F = 0.01$, which has a solution of $q = 0.71$. Other cases are very similar. The azimuthal angle θ in the plot corresponds to the polar angle between \mathbf{p} and \mathbf{q} in the spherical coordinates in which we align \mathbf{q} along the \hat{z} direction. It is evident that the rotational SO(3) symmetry is broken. And *most importantly, the $\mathbf{p} = \mathbf{q}$ point is a saddle point rather than the global minimum of the pair energy.* An alternative plot at unitarity and counterpart plots for the near-BCS and near BEC cases are shown in Supplementary Figs. S1 and S2, respectively.

To see this more clearly, we plot in Fig. 3 the pair dispersion $\Omega_{p=q}$ as a function of the polar angle θ , i.e., along the (constant radius) $p = q$ circle (in Fig. 2), as shown by the black solid line. At the same time, we also show the near-BCS case (red dashed line) at $1/k_F a = -1/2$ with $\eta = 0.4$ and $T/T_F = 0.01$, as well as the ${}^6\text{Li}$ - ${}^{40}\text{K}$ mixture case (blue dotted line) in the BCS regime with $1/k_F a = -1$, $\eta = -0.4$ and $T/T_F = 0.025$. In all cases, we find that the $\mathbf{p} = \mathbf{q}$ point is not the global minimum of the pair dispersion, in contradiction to our assumption that the FFLO state is a spontaneously broken symmetry state. This means that the FFLO

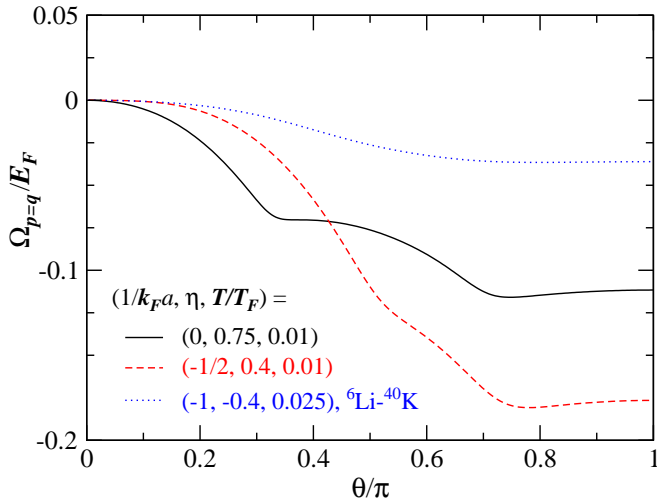


Figure 3. Pair energy $\Omega_{p=q}$ as a function of the polar angle θ , i.e., along the bottom circle in the 3D plot shown in Fig. 2 (black solid line). Also shown are the near-BCS case (red dashed line) at $1/k_F a = -1/2$ and $T/T_F = 0.01$ with (equal mass and) population imbalance $\eta = 0.4$, as well as the ${}^6\text{Li}$ - ${}^{40}\text{K}$ mixture case (blue dotted line) in the BCS regime with $1/k_F a = -1$, $\eta = -0.4$ and $T/T_F = 0.025$. For the latter case, the light species ${}^6\text{Li}$ is the majority.

states found at the mean-field level are *not* stable once pairing fluctuations are taken into account.

To make sure that this finding is not an artifact of the G_0G scheme of our T -matrix theory, we perform similar calculations using our main competitor, the GG scheme of the T -matrix theory, with $\chi_{GG}(P) = \sum_{K\sigma} G_\sigma(P-K)G_{\bar{\sigma}}(K)/2$. This has been known as the FLEX approximation [41], and have been used by various authors in the study of BCS-BEC crossover. Then we compare the results between these two schemes.

Shown in Fig. 4 are representative pair dispersions Ω_p as a function of p along different polar angles θ for both schemes, as labeled in the figure. To be specific, we show the same unitary case as in Fig. 2. The corresponding 3D plot of the pair dispersion from the GG scheme is given in Supplementary Fig. S3. For both schemes, we plot the curves for $\theta = 0$ (black), $\pi/2$ (red) and π (blue). Since the GG scheme (dashed lines) is inconsistent with the mean-field BCS gap equation so that $U^{-1} + \chi_{GG}(0, \mathbf{q}) \neq 0$, its pair dispersion along $\theta = 0$ does *not* touch zero at its minimum, unlike our G_0G case (solid lines). Nevertheless, common to both schemes is that the minimum pair energy along $\theta = 0$ is higher than along other directions, and is thus *not* a global minimum.

By relaxing Eq. (5), one may also study how a finite q progressively leads to an angle dependence of the minimum of Ω_p , as shown in Supplementary Fig. S4.

An unstable mean-field Sarma solution also exists in the mean-field FFLO regime, with a typical pair dispersion shown in the inset of Fig. 4 at high population imbalance. Here $\Omega_{\mathbf{p}=0}$ vanishes, as determined by the gap equation. However, the

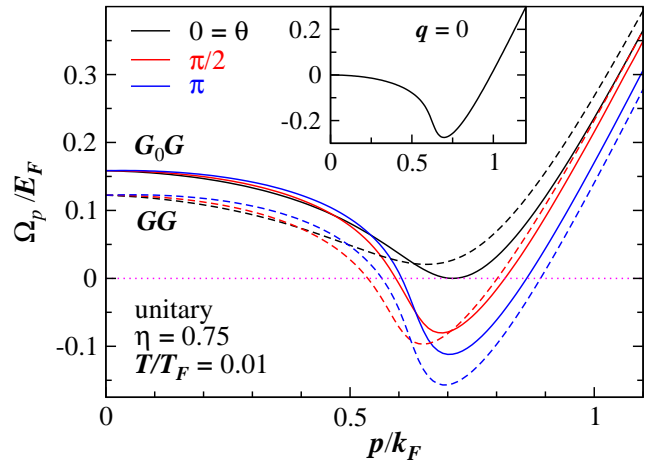


Figure 4. Pair dispersion Ω_p in the mean-field FFLO phase of a mass-balanced unitary Fermi gas with $\eta = 0.75$ as a function of p along different polar angles $\theta = 0$ (black), $\pi/2$ (red), and π (blue), for both the G_0G (solid lines) and GG (dashed lines) schemes of T -matrix theories. For neither scheme, the minimum energy along the \mathbf{q} direction is the global minimum. Here the specific parameters are labeled. Shown in the inset is the pair dispersion with the same parameters but assuming a mean-field Sarma solution, for which $\mathbf{q} = 0$.

pair energy reaches a minimum at a finite p on a 2D sphere \mathbb{S}^2 in the momentum space, which will destroy the mean-field Sarma states. Most importantly, these pairs will never Bose condense, and thus no symmetry breaking or phase transition will occur. In this way, we have shown that the FFLO phase will never occur in 3D continuum, as mentioned earlier. Indeed, setting μ_{pair} to the bottom of the pair energy would lead to a diverging noncondensed pair density, $n_{pair} = a_0 \Delta_{pg}^2$ via Eq. (7), and thus destroy superfluidity. Obviously, this divergence does not rely on the rotational symmetry and can be readily extended to the case of optical lattices.

For a 2D case, there is no true long range order of superfluidity, which is valid for zero momentum condensate. The dimensionality would be reduced to 1D, leading to even stronger fluctuation effects, which shall destroy FFLO type of superfluidity.

Similar instability of the FFLO states is also expected from the G_0G_0 scheme of T -matrix approximation, as in the Nozieres–Schmitt-Rink theory [42]. It is easy to show that the pair dispersion in the mean-field FFLO regime minimizes at a finite q , as shown in Supplementary Fig. S3. Indeed, using such a theory, Ohashi also find that the FF state is unstable in 3D homogeneous Fermi gases for a similar reason [43].

While our calculations were done with the FF states, we argue that such dimensional reduction effects hold for the LO and higher order FFLO states as well. We shall also point out that the pairing field is different from magnetic spin fluctuations, where unlike the pair momentum, the magnitude of a spin is fixed so that spontaneous symmetry breaking may occur as in a non-linear sigma model.

The reason FFLO states are unstable can be understood

from a different perspective. At the mean-field level, it is known that the LO states has *slightly* lower energy than the corresponding FF states. While the FF states are condensation of Cooper pairs at a single momentum q , the LO states are condensation at a pair of momenta $\pm q$. It is conceivable that condensation at two pairs of q 's forming a square in the momentum space shall further lower the energy, as has been confirmed by mean-field calculations [44]. Along the same line, it suggests that condensation at 3, 4, 6, and 8 pairs of momenta and so on should have a progressively lower energy. Eventually, it leads to the conclusion that the lowest energy solution would be condensation on the entire 2D constant-energy surface, on which the pair dispersion minimizes. This is, of course, no longer a condensed state, nor an FFLO state. We note that these mean-field crystalline states are different from ordinary spontaneous breaking of the SO(3) symmetry, which typically has only one preferential direction, as one finds in textbooks.

Finally, we investigate the nature of this unusual normal state, for which the pair dispersion Ω_p minimizes at finite p . The pairing correlation function for the 3D continuum case is given by

$$C(r) \propto \int \frac{e^{i\mathbf{p}\cdot\mathbf{r}} d^3p}{\xi^2(p-q)^2 + \tau} \approx \frac{1}{4\pi r \xi^2} \sqrt{\frac{4\xi^2 q^2 + \tau}{\tau}} e^{-r\sqrt{\tau}/\xi} \sin(qr), \quad (8)$$

where $\xi^2 = a_0 B_{\parallel}$ is the screening length (squared), and $\tau = -a_0 \mu_{pair} > 0$, with $\mu_{pair} \propto T$ near zero T . (Note here that the pair dispersion is isotropic). Apart from the oscillating behavior, the correlation length is given by $\xi/\sqrt{\tau} \propto \xi/\sqrt{T}$. When $T \rightarrow 0$, the exponential decay will disappear, leaving a r^{-1} power law decay at large distances so that the pairs approach an algebraic Bose liquid. Note that this oscillating behavior due to a finite q is very unusual, manifesting the tendency to form a wave-like pairing order. Without superfluidity, such a Bose liquid is a Bose metal in the ground state, where μ_{pair} approaches 0 at zero T . Of course, at high population imbalance, the major part of the system is composed of the excessive majority fermions, which add to the metallic character of the system. We shall call this phase ‘‘anomalous metal’’.

Recently, Radzihovsky and Vishwanath[45] found that the LO phase is unstable, which is consistent with our findings here. Further on, they continued with the unstable LO state and concluded that fermion pairs may pair again to form a nematic charge-4 SF₄ superfluid phase. However, because the interaction between fermion pairs are usually repulsive, it is unlikely that such an SF₄ phase will form.

As of this writing, Boyack et al [46] found that the superfluid density of a mean-field FF state vanishes in the direction transverse to the wavevector \mathbf{q} , in agreement with our findings here.

There have also been theoretical studies of possible FFLO (or stripe) states in Fermi gases with spin-orbit coupling

[47, 48]. We point out that the spin-orbit coupling forces a preferential direction, and/or leads to topologically distinct Fermi surfaces, making the system drastically different from the conventional FFLO physics. There are also studies of FFLO phases in 1D Fermi gases, which, however, does not process long range order at all.

In summary, we have studied the effects of pairing fluctuations on the mean-field FFLO phases, and found that FFLO phases are intrinsically unstable against pairing fluctuations in both continuum and optical lattices in 3D and 2D, and thus do not exist experimentally. This conclusion holds on general physical grounds, independent of our specific pairing fluctuation theory, and is applicable for both quantum gases and condensed matter systems.

We thank A.J. Leggett, K. Levin and S.Z. Zhang for helpful discussions. This work is supported by NSF of China (Grant No. 11274267), the National Basic Research Program of China (Grants No. 2011CB921303 and No. 2012CB927404), NSF of Zhejiang Province of China (Grant No. LZ13A040001).

* Corresponding author: qchen@zju.edu.cn

- [1] Fulde, P. & Ferrell, R. A. Superconductivity in a strong spin-exchange field. *Phys. Rev.* **135**, A550–A563 (1964).
- [2] Larkin, A. I. & Ovchinnikov, Y. N. Inhomogeneous state of superconductors. *Sov. Phys. JETP* **20**, 762–769 (1965). [*Zh. Eksp. Teor. Fiz.* **47**, 1136 (1964)].
- [3] Casalbuoni, R. & Nardulli, G. Inhomogeneous superconductivity in condensed matter and QCD. *Rev. Mod. Phys.* **76**, 263–320 (2004).
- [4] Radovan, H. A. *et al.* Magnetic enhancement of superconductivity from electron spin domains. *Nature* **425**, 51–55 (2003).
- [5] Kenzelmann, M. *et al.* Coupled superconducting and magnetic order in CeCoIn₅. *Science* **321**, 1652–1654 (2008).
- [6] Shimahara, H. Fulde-Ferrell-Larkin-Ovchinnikov state and field-induced superconductivity in an organic superconductor. *J. Phys. Soc. Jpn.* **71**, 1644 (2002).
Lebed, A. G. & Wu, S. Larkin-Ovchinnikov-Fulde-Ferrell phase in the superconductor (TMTSF)₂ClO₄: Theory versus experiment. *Phys. Rev. B* **82**, 172504 (2010).
- [7] Vorontsov, A. B., Sauls, J. A. & Graf, M. J. Phase diagram and spectroscopy of FFLO states of two-dimensional d -wave superconductors. *Phys. Rev. B* **72**, 184501 (2005).
Wang, Q., Chen, H.-Y., Hu, C.-R. & Ting, C. S. Local tunneling spectroscopy as signatures of the Fulde-Ferrell-Larkin-Ovchinnikov state in s - and d -wave superconductors. *Phys. Rev. Lett.* **96**, 117006 (2006).
Berridge, A. M., Green, A. G., Grigera, S. A. & Simons, B. D. Inhomogeneous magnetic phases: a LOFF-like phase in Sr₃Ru₂O₇. *Phys. Rev. Lett.* **102**, 136404 (2009).
Cho, K. *et al.* Anisotropic upper critical field and a possible Fulde-Ferrel-Larkin-Ovchinnikov state in a stoichiometric pnictide superconductor LiFeAs. *Phys. Rev. B* **83**, 060502R (2011).
Ptok, A. & Crivelli, D. The Fulde-Ferrell-Larkin-Ovchinnikov state in pnictides. *J. Low Temp. Phys.* **172**, 226 (2013).
- [8] MÜther, H. & Sedrakian, A. Phases of asymmetric nuclear matter with broken space symmetries. *Phys. Rev. C* **67**, 015802

- (2003).
- [9] Alford, M., Bowers, J. & Rajagopal, K. Crystalline color superconductivity. *Phys. Rev. D* **63**, 074016 (2001).
Bowers, J. A. & Rajagopal, K. The crystallography of color superconductivity. *Phys. Rev. D* **66**, 065002 (2002).
- [10] Sedrakian, A., Mur-Petit, J., Polls, A. & Mütter, H. Pairing in a two-component ultracold Fermi gas: phases with broken space symmetries. *Phys. Rev. A* **72**, 013613 (2005).
Liao, Y.-A. *et al.* Spin-imbalance in a one-dimensional Fermi gas. *Nature* **467**, 567–569 (2010).
Radzihovsky, L. & Sheehy, D. E. Imbalanced Feshbach-resonant Fermi gases. *Rep. Prog. Phys.* **73**, 076501 (2010).
- [11] Gloos, K. *et al.* Possible formation of a nonuniform superconducting state in the heavy-fermion compound UPd₂Al₃. *Phys. Rev. Lett.* **70**, 501–504 (1993).
- [12] Huxley, A. D. *et al.* Flux pinning, specific heat and magnetic properties of the laves phase superconductor CeRu₂. *J. Phys. Condens. Matter* **5**, 7709 (1993).
- [13] Norman, M. R. Existence of the FFLO state in superconducting UPd₂Al₃. *Phys. Rev. Lett.* **71**, 3391 (1993).
- [14] Tenya, K. *et al.* Field-history-dependent peak effect in the superconducting mixed state of CeRu₂. *Physica B: Condens. Matter* **259-261**, 692–693 (1999).
- [15] Chen, Q. J., Stajic, J., Tan, S. N. & Levin, K. BCS-BEC crossover: From high temperature superconductors to ultracold superfluids. *Phys. Rep.* **412**, 1–88 (2005).
- [16] Bloch, I., Dalibard, J. & Zwerger, W. Many-body physics with ultracold gases. *Rev. Mod. Phys.* **80**, 885–964 (2008).
- [17] He, Y., Chien, C.-C., Chen, Q. J. & Levin, K. Single-plane-wave Larkin-Ovchinnikov-Fulde-Ferrell state in BCS-BEC crossover. *Phys. Rev. A* **75**, 021602 (2007).
- [18] Sheehy, D. E. & Radzihovsky, L. BEC-BCS crossover in “magnetized” Feshbach-resonantly paired superfluids. *Phys. Rev. Lett.* **96**, 060401 (2006).
- [19] Hu, H. & Liu, X.-J. Mean-field phase diagrams of imbalanced Fermi gases near a Feshbach resonance. *Phys. Rev. A* **73**, 051603 (2006).
- [20] He, L., Jin, M. & Zhuang, P. Finite-temperature phase diagram of a two-component Fermi gas with density imbalance. *Phys. Rev. B* **74**, 214516 (2006).
- [21] Combescot, R. & Mora, C. Transition to the Fulde-Ferrell-Larkin-Ovchinnikov planar phase : A quasiclassical investigation with Fourier expansion. *Phys. Rev. B* **71**, 144517 (2005).
Yoshida, N. & Yip, S.-K. Larkin-Ovchinnikov state in resonant Fermi gas. *Phys. Rev. A* **75**, 063601 (2007).
- [22] Wang, J. B., Che, Y. M., Zhang, L. F. & Chen, Q. J. Enhancement effect of mass imbalance on Fulde-Ferrell-Larkin-Ovchinnikov type of pairing in Fermi-Fermi mixtures of ultracold quantum gases. *Sci. Rep.* **7**, 39783 (2017).
- [23] Machida, K., Mizushima, T. & Ichioka, M. Generic phase diagram of fermion superfluids with population imbalance. *Phys. Rev. Lett.* **97**, 120407 (2006).
- [24] Zhang, W. & Duan, L.-M. Finite-temperature phase diagram of trapped Fermi gases with population imbalance. *Phys. Rev. A* **76**, 042710 (2007).
- [25] Kinnunen, J., Jensen, L. M. & Törmä, P. Strongly interacting Fermi gases with density imbalance. *Phys. Rev. Lett.* **96**, 110403 (2006).
- [26] Zwierlein, M. W., Schirotzek, A., Schunck, C. H. & Ketterle, W. Fermionic superfluidity with imbalanced spin populations. *Science* **311**, 492 (2006).
- [27] Partridge, G. B., Li, W., Kamar, R. I., Liao, Y. A. & Hulet, R. G. Pairing and phase separation in a polarized Fermi gas. *Science* **311**, 503 (2006).
- [28] Gubbels, K. B., Baarsma, J. E. & Stoof, H. T. C. Lifshitz point in the phase diagram of resonantly interacting ⁶Li-⁴⁰K mixtures. *Phys. Rev. Lett.* **103**, 195301 (2009).
Baarsma, J. E., Gubbels, K. B. & Stoof, H. T. C. Population and mass imbalance in atomic Fermi gases. *Phys. Rev. A* **82**, 013624 (2010).
- [29] Baarsma, J. E. & Stoof, H. T. C. Inhomogeneous superfluid phases in ⁶Li-⁴⁰K mixtures at unitarity. *Phys. Rev. A* **87**, 063612 (2013).
- [30] Cai, Z., Wang, Y. & Wu, C. Stable Fulde-Ferrell-Larkin-Ovchinnikov pairing states in 2D and 3D optical lattices. *Phys. Rev. A* **83**, 063621 (2011).
Franca, V. V., Hördlein, D. & Buchleitner, A. Fulde-Ferrell-Larkin-Ovchinnikov critical polarization in one-dimensional fermionic optical lattices. *Phys. Rev. A* **86**, 033622 (2012).
Mendoza, R., Fortes, M., Solís, M. A. & Koinov, Z. Superfluidity of a spin-imbalanced Fermi gas in a three-dimensional optical lattice. *Phys. Rev. A* **88**, 033606 (2013).
Okawauchi, Y. & Koga, A. Stability of FFLO states in optical lattices with bilayer structure. *J. Phys. Soc. Jpn.* **81**, 074001 (2012).
Kim, D.-H. & Törmä, P. Fulde-Ferrell-Larkin-Ovchinnikov state in the dimensional crossover between one- and three-dimensional lattices. *Phys. Rev. B* **85**, 180508(R) (2012).
Chen, A.-H. & Gao, X. L. Pure Fulde-Ferrell-Larkin-Ovchinnikov state in optical lattices. *Phys. Rev. B* **85**, 134203 (2012).
- [31] Chen, Q. J., Kosztin, I., Jankó, B. & Levin, K. Pairing fluctuation theory of superconducting properties in underdoped to overdoped cuprates. *Phys. Rev. Lett.* **81**, 4708–11 (1998).
- [32] When pairing is so strong that a two-body bound state with a large binding energy forms in the real space, the momenta of the component fermions in the pair will span a large momentum space. In this case, the Pauli exclusion between the component fermions and the Fermi sphere is weak, and the pair will happily coexist with the Fermi sea, with a dispersion minimizing at zero momentum.
- [33] Chen, Q. J., Stajic, J. & Levin, K. Applying BCS-BEC crossover theory to high temperature superconductors and ultracold atomic Fermi gases. *Low Temp. Phys.* **32**, 406 (2006). [Fiz. Nizk. Temp. **32**, 538 (2006)].
- [34] Chen, Q. J., He, Y., Chien, C.-C. & Levin, K. Theory of radio frequency spectroscopy experiments in ultracold Fermi gases and their relation to photoemission experiments in the cuprates. *Rep. Prog. Phys.* **72**, 122501 (2009).
- [35] Chien, C. C., Chen, Q. J., He, Y. & Levin, K. Intermediate temperature superfluidity in a Fermi gas with population imbalance. *Phys. Rev. Lett.* **97**, 090402 (2006).
- [36] Chen, Q. J., He, Y., Chien, C.-C. & Levin, K. Theory of superfluids with population imbalance: Finite-temperature and BCS-BEC crossover effects. *Phys. Rev. B* **75**, 014521 (2007).
- [37] Guo, H., Chien, C.-C., Chen, Q. J., He, Y. & Levin, K. Finite-temperature behavior of an interspecies fermionic superfluid with population imbalance. *Phys. Rev. A* **80**, 011601 (2009).
- [38] Wang, J. B., Guo, H. & Chen, Q. J. Exotic phase separation and phase diagrams of a Fermi-Fermi mixture in a trap at finite temperature. *Phys. Rev. A* **87**, 041601 (2013).
- [39] Pao, C.-H., Wu, S.-T. & Yip, S.-K. Superfluid stability in the BEC-BCS crossover. *Phys. Rev. B* **73**, 132506 (2006).
- [40] Chen, Q. J., He, Y., Chien, C.-C. & Levin, K. Stability conditions and phase diagrams for two-component Fermi gases with population imbalance. *Phys. Rev. A* **74**, 063603 (2006).
- [41] Bickers, N. E., Scalapino, D. J. & White, S. R. Conserving approximations for strongly correlated electron systems: Bethe-

- Salpeter equation and dynamics for the two-dimensional Hubbard model. *Phys. Rev. Lett.* **62**, 961–964 (1989).
- [42] Nozières, P. & Schmitt-Rink, S. Bose condensation in an attractive fermion gas: from weak to strong coupling superconductivity. *J. Low Temp. Phys.* **59**, 195–211 (1985).
- [43] Ohashi, Y. On the Fulde-Ferrell state in spatially isotropic superconductors. *J. Phys. Soc. Jpn.* **71**, 2625 (2002).
- [44] Zhang, S. Z. Private communications.
- [45] Radzihovsky, L. & Vishwanath, A. Quantum liquid crystals in an imbalanced Fermi gas: Fluctuations and fractional vortices in Larkin-Ovchinnikov states. *Phys. Rev. Lett.* **103**, 010404 (2009).
- [46] Boyack, R., Wu, C.-T., Anderson, B. M. & Levin, K. Collective mode contributions to the Meissner effect: Fulde-Ferrell and pair-density wave superfluids (2017). Unpublished.
- [47] Zheng, Z., Gong, M., Zou, X., Zhang, C. & Guo, G. Route to observable Fulde-Ferrell-Larkin-Ovchinnikov phases in three-dimensional spin-orbit-coupled degenerate Fermi gases. *Phys. Rev. A* **87**, 031602 (2013).
- Liu, X.-J. & Hu, H. Inhomogeneous Fulde-Ferrell superfluidity in spin-orbit-coupled atomic Fermi gases. *Phys. Rev. A* **87**, 051608(R) (2013).
- [48] Dong, L., Jiang, L. & Pu, H. Fulde-Ferrell pairing instability in spin-orbit coupled Fermi gas. *New J. Phys.* **15**, 075014 (2013).
- Iskin, M. Spin-orbit coupling induced Fulde-Ferrell-Larkin-Ovchinnikov-like Cooper pairing and skyrmion-like polarization textures in trapped optical lattices. *Phys. Rev. A* **88**, 013631 (2013).
- Wu, F., Guo, G.-C., Zhang, W. & Yi, W. Unconventional superfluid in a two-dimensional Fermi gas with anisotropic spin-orbit coupling and Zeeman fields. *Phys. Rev. Lett.* **110**, 110401 (2013).

Supplementary Information

Instability of Fulde-Ferrell-Larkin-Ovchinnikov states in three and two dimensions

Jibiao Wang, Yanming Che, Leifeng Zhang and Qijin Chen*

Department of Physics and Zhejiang Institute of Modern Physics, Zhejiang University,

Hangzhou, Zhejiang 310027, China and

Synergetic Innovation Center of Quantum Information and Quantum Physics, Hefei, Anhui

230026, China

Here we provide more data and plots, which serve as supplemental information to the main text.

PAIR DISPERSION IN THE MEAN-FIELD FFLO PHASES FROM NEAR-BCS THROUGH NEAR-BEC REGIMES

In this section, we will present more results of the pair dispersion at high population imbalances in the *mean-field* FFLO phase from near-BCS through near-BEC regimes.

Starting with the unitary case, Fig. S1 shows the pair dispersion $\Omega_{\mathbf{p}}$ in the FFLO phase with a population imbalance $\eta = 0.75$ and equal masses at temperature $T/T_F = 0.01$. This is just an alternative 3D plot of Fig. 2 in the main text, treating the angle θ between pair momentum \mathbf{p} and the FFLO wavevector \mathbf{q} as a Descartes coordinate. This makes it easier to see that the minimum value of Ω_p (as a function of p) decreases as θ varies from 0 to π , revealing that the point $\mathbf{p} = \mathbf{q}$ is indeed merely a saddle point of $\Omega_{\mathbf{p}}$.

Now we show the counterpart plot of the near-BCS and near-BEC cases in Fig. S2, as the left and right panel, respectively. Despite the different radii of the bottom (half) circle, both confirms that the $\mathbf{p} = \mathbf{q}$ point is a saddle point of $\Omega_{\mathbf{p}}$.

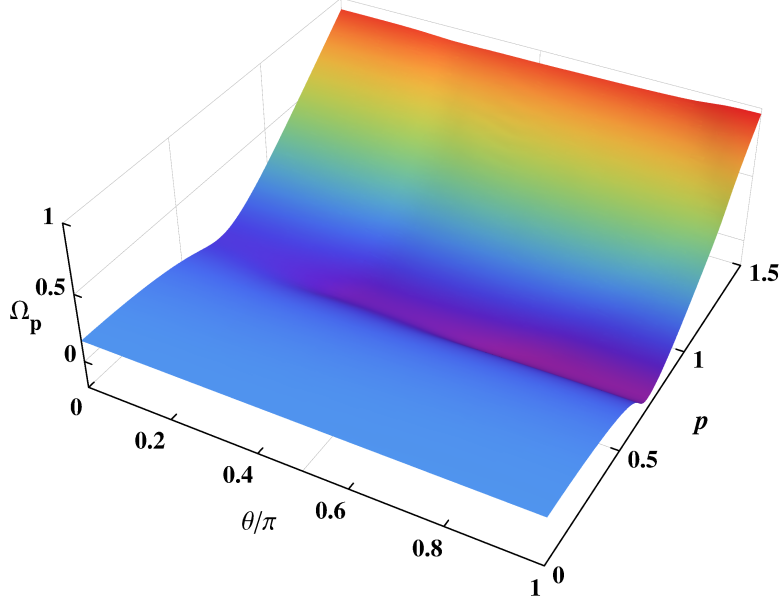


Figure S1. Alternative 3D plot of the pair dispersion Ω_p in the FFLO phases at unitarity with population imbalance $\eta = 0.75$ and temperature $T/T_F = 0.01$. The conventions on color coding and units are the same as in Fig. 2 of the main text.

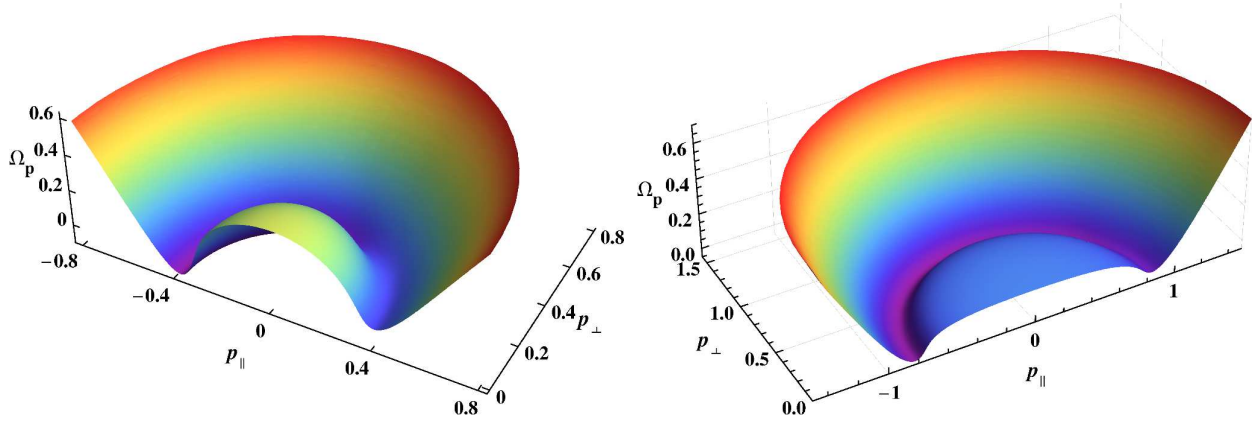


Figure S2. Pair dispersion Ω_p in the FFLO phases for the near-BCS and near-BEC case, with $(1/k_F a, \eta, T/T_F) = (-1/2, 0.45, 0.01)$ and $(0.1, 0.75, 0.01)$ for the left and right panels, respectively. The conventions on color coding and units are the same as in Fig. 2 of the main text.

PAIR DISPERSION FROM THE GG AND G_0G_0 APPROXIMATIONS OF PAIRING FLUCTUATION THEORIES

Similar to the G_0G scheme of the T -matrix approximation, one can also extract the pair dispersion from the counterpart T matrix in the GG and G_0G_0 schemes. The derivation is straight

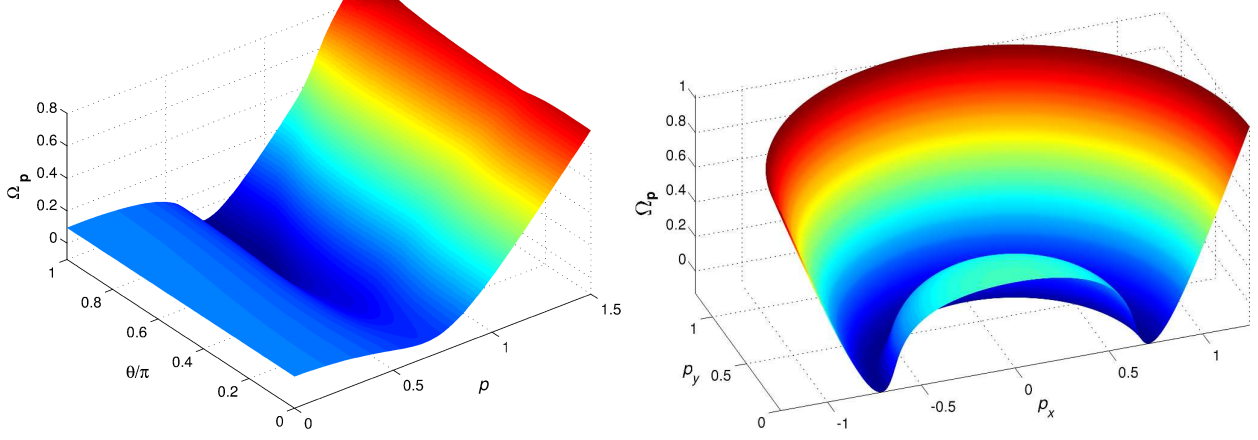


Figure S3. Typical pair dispersion $\Omega_{\mathbf{p}}$ in the mean-field FFLO phases for the (left) GG and (right) G_0G_0 approximations of the pairing fluctuation theories. Shown here is the unitary case with $\eta = 0.75$ and $T/T_F = 0.01$. The conventions on color coding and units are the same as in Fig. 2 of the main text.

forward, using by setting frequency Ω to zero in the inverse T matrix, as discussed above Eq. (7) in the main text. With no doubt, the coefficient a_0 is quantitatively different. To make different plots comparable in numerical values, we use the a_0 from the G_0G scheme to plot the pair dispersion here. Note that one could equivalently plot $-1/U + \chi(0, \mathbf{p})$ rather than $\Omega_{\mathbf{p}}$ instead. The resulting pair dispersion at unitarity is shown in Fig. S3 for the (left) GG and (right) G_0G_0 schemes, respectively. Here values of the chemical potentials μ_{σ} , the gap Δ , and the vector \mathbf{q} were the same as in Fig. 2 in the main text for the G_0G case.

Evidently, the pair dispersion for the GG case is similar to that of the G_0G case, confirming that the $\mathbf{p} = \mathbf{q}$ point is a saddle point of $\Omega_{\mathbf{p}}$. In contrast, there is an obvious difference between the G_0G_0 case and the other two; the pair dispersion has no angle dependence. This can be easily understood since the pair susceptibility $\chi_0(P) = \sum_K G_0(P-K)G_0(K)$ is isotropic, independent of the gap Δ and the wavevector \mathbf{q} . This is, of course, the defect of the approximation. Nevertheless, this angle independence does suggest that the pair energy minimizes on a finite momentum sphere so that no spontaneous symmetry breaking or Bose condensation would take place for the pairs.

Note that the pair dispersion for the GG and G_0G_0 schemes does not vanish at $\mathbf{p} = \mathbf{q}$, because these two schemes are incompatible with the BCS mean-field gap equation.

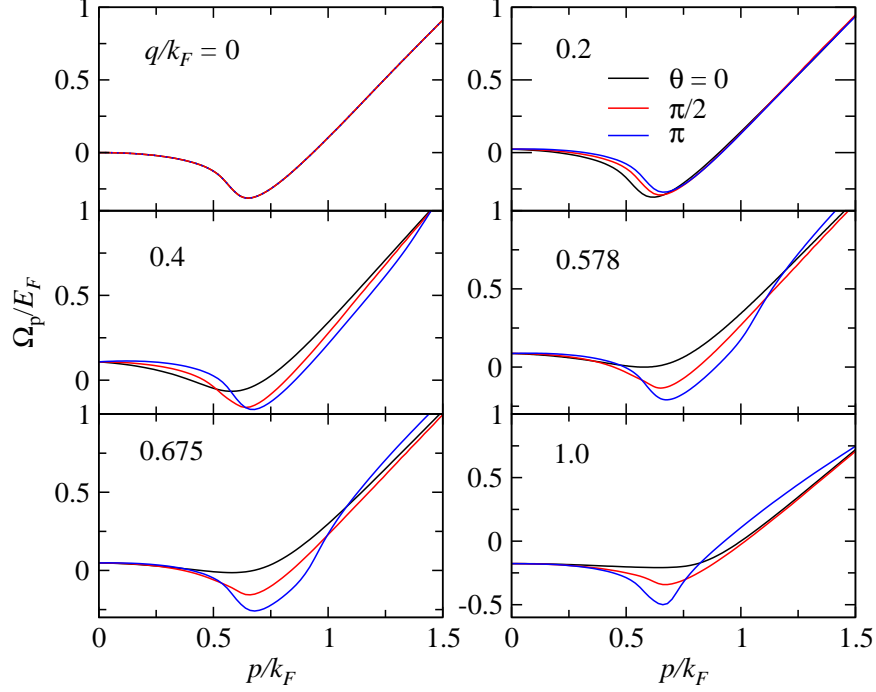


Figure S4. Evolution of the pair dispersion $\Omega_{\mathbf{p}}$ at different angles in the mean-field FFLO phases with increasing wavevector q , as labeled. Shown here is the unitary case with $\eta = 0.6$ at $T/T_F = 0.01$.

EVOLUTION OF PAIR DISPERSION WITH A FORCED LOFF WAVEVECTOR \mathbf{q}

It is illuminating to show how the pairing dispersion evolves if one forces and continuously tunes the FFLO wavevector \mathbf{q} , starting from the Sarma solution in a mean-field FFLO phase. This can be done by solving Eqs. (2)-(4) in the main text, without Eq. (5). Here we work with our own pairing fluctuation theory, i.e., the G_0G approximation. The result is shown in Fig. S4 for $\eta = 0.6$ at unitarity. For $q = 0$, i.e., the Sarma state, the pair dispersion vanishes at zero momentum, and is isotropic with no angle dependence. The solution for $q/k_F = 0.578$ corresponds to the mean-field FF solution. As one can see, angle dependence develops as q increases from 0. In all finite q cases, the minimum pair energy along the \mathbf{q} direction is the highest among all angles. And therefore, these finite q FFLO states are unstable against pairing fluctuations.